# 2

# Ultrasonic Projection

Krzysztof J. Opieliński
*Institute of Telecommunications, Teleinformatics and Acoustics,*
*Wroclaw University of Technology*
*Poland*

## 1. Introduction

Ultrasonic technique of imaging serves an increasingly important role in medical diagnostics. In most of applications, echographic methods are used (ultrasonography, ultrasonic microscopy). Using such methods, an image presenting changes of a reflection coefficient in the interior of analysed structure is being constructed. This chapter presents possibilities of utilising information included in ultrasonic pulses, which penetrate an object in order to create images presenting the projection of analysed structure (Opielinski & Gudra, 2004b, 2004c, 2005, 2006, 2008, 2010a, 2010b, 2010c; Opielinski et al., 2009, 2010a, 2010b) in the form of a distribution of mean values of a measured acoustic parameter, for one or numerous planes, perpendicular to the direction of ultrasonic waves incidence (analogical as in X-ray radiography). Due to the possibility of obtaining images in pseudo-real time, the device using this method was named the ultrasonic transmission camera (UTC) (Ermert et al., 2000). Only some centres in the world work on this issue and there are a low number of laboratory research setups, which enable pseudo-real time visualisation of biological structures using UTC: Stanford Research Institute in USA (Green et al., 1974; Green et al., 1976), Gesellschaft für Strahlen- und Umweltforschung at Neuherberg in Germany (Brettel et al., 1981; Brettel et al., 1987), Siemens Corporate Technology in Germany (Ermert et al., 2000; Granz & Oppelt, 1987; Keitmann et al., 2002), Wroclaw University of Technology in Poland (Opielinski & Gudra, 2000; Opielinski & Gudra, 2005, Opielinski et al., 2010a, 2010b), University of California in San Diego and University of Washington Medical Center in Seattle (Lehmann et al., 1999). In most of studies, the projection parameter is the signal amplitude, not its transition time, which seems to more attractive due to the simplicity and precision of measurements. The majority of 2-D ultrasonic multi-element matrices are designed for miniature 3-D volumetric medical endoscopic imaging as intracavital probes provided unique opportunities for guiding surgeries or minimally invasive therapeutic procedures (Eames & Hossack, 2008; Karaman et al., 2009; Wygant et al., 2006a; Wygant et al., 2006b). It can be concluded based on worldwide literature review that most of the 2-D ultrasonic matrices are assigned to work of echo method (Drinkwater & Wilcox, 2006). Moreover, the commercial devices (e.g. Submersible Ultrasonic Scanning Camera made of Matec Micro Electronics, AcoustoCam produced by Imperium Inc.) work using reflection method and are designed for non-destructive inspection (NDI), most of all. It allows manufacturers to instantly visualize a variety of material subsurface faults (voids, delaminating, cracks and corrosion).

This chapter, with the use of a computer simulation and real measurements, includes the complex analysis of the precision of images obtained using visualisation of mean values of sound speed and a frequency derivative of the ultrasonic wave amplitude attenuation coefficient (by the means of measurements of the transition time and the frequency down shift projection values of transmitted ultrasonic pulses) from the point of view of possibilities of using UTC for visualisation of biological structures, especially for soft tissue examinations (*in vivo* female breast). The principles of ultrasonic projection methods are described at the beginning (Section 2), and then the projections of acoustic parameters are clearly defined (Section 3). Section 4 contains theoretical analysis of ultrasonic projection method accuracy. By the means of elaborated software, there was done a simulation of the ultrasonic projection data for several three-dimensional objects immersed in water, what is presented in Section 5, as well as obtained projection images of these objects. The simple measurement setup for examining biological structures by the means of ultrasonic projection, in the set of single-element ultrasonic sending and receiving probes and projection measurement results are presented in Section 6. Next, the construction, parameters and operating way of three different types of ultrasonic 2-D flat multi-element matrices (standard, passive and active one) elaborated by the author and his team, are described (Section 7). The models of ultrasonic transmission camera were constructed in the result, what is presented in Section 8. The conclusion (Section 9) contains a summary and the plane for the future to improve the quality of ultrasonic projection images and increase scanning resolution.

## 2. Ultrasonic projection methods

Analogically as in case of X-ray pictures (RTG - roentgenography), for visualisation of biological structures, it is possible to use the projection method with utilisation of ultrasonic waves. In case of generating of ultrasonic plane waves (parallel beam rays), we shall obtain an image in the parallel projection and in case of generating of ultrasonic spherical waves (divergent beam rays), it shall be an image in the central projection; it is also possible to use a source of cylindrical waves (beam rays are divergent on one plane and parallel in perpendicular plane) – central-parallel projection (Fig.1) (Opielinski & Gudra, 2004c).

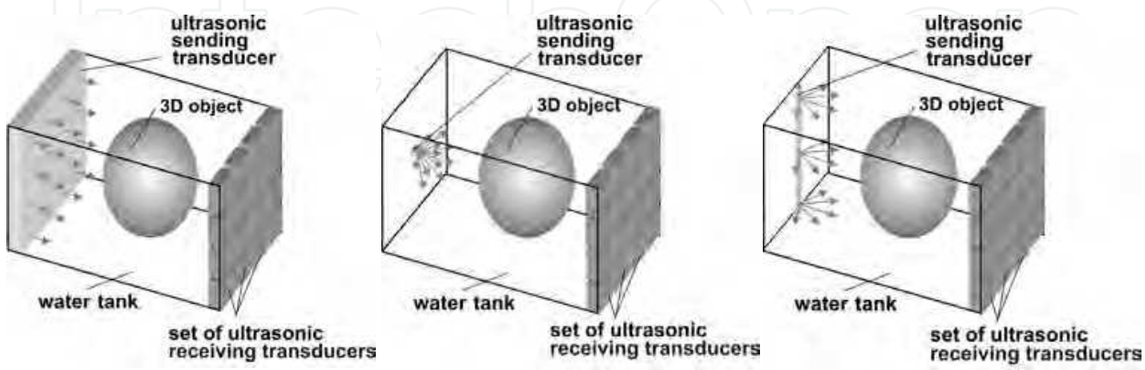


(a) (b) (c)

Fig. 1. The way of visualization of a biological structure by means of the ultrasonic projection: a) parallel, b) central (divergent), c) central–parallel (divergent–parallel)

Phenomena related with propagation of ultrasonic waves in biological structures (diffusion, diffraction, interference, refraction and reflection) induce small distortions of a projection image, if the local values of acoustic impedance in an examined structure are not significantly diversified (Opielinski & Gudra, 2000). The greatest advantage of ultrasonic diagnostics is its non-invasiveness, by dint of which, it is possible to attain a multiple projection of an examined biological structure at numerous different directions *in vivo*, what enables a three-dimensional reconstruction of heterogeneity borders in its interior (Opielinski & Gudra, 2004a).

By the means of using the transmission method, it is also possible to obtain a twice higher level of amplitude of ultrasonic receiving pulses in comparison with the echo method. In this case, the subject of imaging can simultaneously be several acoustic parameters, digitally determined on the basis of information directly contained in ultrasonic pulses, which penetrate a biological structure (e.g. amplitude, transition time, mid-frequency down shift, spectrum of receiving pulse). Such method enables obtaining various projection images, every of which characterises slightly different traits of a structure (e.g. distribution of mean (projective) values of attenuation coefficient and propagation velocity of ultrasonic waves, frequency derivative of attenuation coefficient, nonlinear acoustic parameter $B/A$ (Greenleaf & Sehgal, 1992; Kak & Slaney, 1988). What is more, if projective measurements of a distribution of a specified acoustic parameter of an examined projection plane of a biological medium, are recorded from numerous directions around the medium, it is possible to reconstruct a distribution of local values of this parameter in 3-D space by determining the inverse Radon transform (Kak & Slaney, 1988; Opielinski & Gudra, 2010b) (ultrasonic transmission tomography). Such complex tomographic characteristics may have a key importance, for example at detecting and diagnosing cancerous changes in soft tissues (e.g. in female breast).

## 3. Projection of acoustic parameters

According to the definition of function projection, projective values of an acoustic parameter, measured at projections, are an integral of their local values, in the path of an ultrasonic beam, transmitted from a source to a detector. Moreover, point sizes of the transmitter and the receiver, the rectilinear path between them and an infinitely narrow ultrasonic wave beam are assumed. It is easy to prove that transition time of an ultrasonic wave is an integer of an inverse of local values of sound velocity through the propagation path $L$ (Opielinski & Gudra, 2010b):

$$t_p = \int_L dt_p = \int_L \frac{dt_p}{dl}\,dl = \int_L \frac{1}{c(x,y,T)}\,dl \tag{1}$$

where $c(x,y,T)$ denotes the sound speed local value at point $(x,y)$ of an object's cross-section on the propagation path, at set temperature $T$, $(dl)^2 = x^2 + y^2$. By a direct measurement of values of transition time of an ultrasonic wave, it is not difficult to image a distribution of projective values of sound velocity $c_p = L/t_p$ in determined plane of projection of a biological medium, immersed in water, assuming the linear propagation path of wave.

By the means of measuring the amplitude of an ultrasonic pulse after a transition through the structure of a biological medium, it is possible to obtain information about the projective

value of an amplitude attenuation coefficient $a_p = ln(A_N/A_L)/L$, measured at the set frequency of a transmitting pulse $f_N$ and temperature $T$ (Opielinski & Gudra, 2010b):

$$\ln\frac{A_N}{A_L} = \int_L \frac{1}{dl}\ln\frac{A(l_i)}{A(l_{i+1})}dl = \int_L \alpha(x,y,f_N,T)dl \tag{2}$$

where $A_N$ – amplitude of an ultrasonic pulse before transition (near the source), $A_L$ – amplitude of an ultrasonic pulse after transition through an object (dipped in water) on the path of $L$, $A(l_i)$ and $A(l_{i+1})$ – amplitudes of an ultrasonic pulse after transition through an object on segments $l_i$ and $l_{i+1}$, respectively, of the path $L$, and distance $dl = l_{i+1} - l_i$. Due to difficulties related with measuring the amplitude $A_N$, it is possible to directly determine the difference of projective values of the amplitude attenuation coefficients $(a_p - a_w) = \ln(A_w/A_L)/L$, where $a_w$ – attenuation coefficient in water, $A_w$ – amplitude of an pulse after passing the path $L$ in water without any biological medium.

Assuming a linear change of attenuation with frequency (as a certain approximation for soft tissues (Kak & Slaney, 1988)), it is possible to obtain an amplitude attenuation coefficient, independent from frequency $a_o(x,y,T)$:

$$\alpha(x,y,T,f) = \left(\alpha_o(x,y,T)\right)\cdot f \tag{3}$$

On this basis, it is possible to use in ultrasonic projection measurements the method of measuring down shifting of mid-frequency of a receiving pulse. After transition of an ultrasonic signal through an object, there is a slight change of its mid-frequency $f_r$, which can be measured by FFT or by a zero-crossing counter (Opielinski & Gudra, 2010b). Then, the projective value of a frequency derivative of an amplitude attenuation coefficient $a_o(x,y,T)$ can be determined in the following form (Kak & Slaney, 1988):

$$\frac{f_N - f_r}{2\sigma^2} = \int_L \alpha_o(x,y,T)dl \tag{4}$$

where variance $\sigma^2$ is the measure of the power spectrum bandwidth of receiving signal after a transition through water. More complex models, e.g. with considering the relationship $a = a_o f^n$, where $n \neq 1$ (in case of soft tissues $1 \leq n \leq 2$), can be found in references (Narayana & Ophir, 1983).

The development of computer technologies enables now also projective measurements of acoustic parameters of biological media, which require time-consuming calculations. One of such parameters is non-linear acoustic parameter $B/A$, which characterises non-linear response of a measured tissue structure on propagation of an ultrasonic wave (Opielinski & Gudra, 2010b). Parameter $B/A$ can be determined by the means of measuring transition times for different static pressures or by measurements of higher harmonics as a distance function (Greenleaf & Sehgal, 1992; Zhang et al., 1997).

## 4. Theoretical analysis of ultrasonic projection method accuracy

The theoretical analysis, which enables estimating of the accuracy of the projective visualisation of heterogeneities in a tissue structure was conducted for a projection of

ultrasonic wave propagation velocity (mean sound velocity on a rectilinear section of the beam path from the source to the detector), obtained after wave's transition through the model of a heterogeneous sphere in its axis (Fig.2) (Opielinski & Gudra, 2004b, 2006).

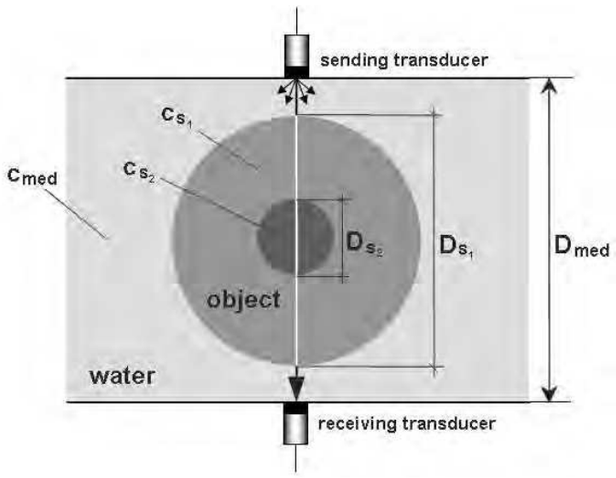


Fig. 2. Theoretical model of a heterogeneous sphere (because of ultrasound propagation speed)

It was assumed that a sphere of the diameter $D_{s1}$ and sound speed $c_{s1}$ = 1500 m/s contains a spherical heterogeneity of the diameter $D_{s2}$ and sound speed $c_{s2}$. It was also assumed that the sound speed in water where the sphere is immersed $c_{med}$ = 1485 m/s (for ~21˚C) and the distance between surfaces of the sending and receiving transducers is $D_{med}$ = 20 cm (simulation of female breast examination). The mean value (projection) of sound speed $c_p$ between surfaces of the transmitter and the receiver was determined using the formula (Opielinski & Gudra, 2004b, 2006):

$$c_p = \frac{D_{med}\, c_{med}\, c_{s1}\, c_{s2}}{c_{s1}\, c_{s2}\left(D_{med} - D_{s1}\right) + c_{med}\, c_{s2}\left(D_{s1} - D_{s2}\right) + c_{med}\, c_{s1}\, D_{s2}} \tag{5}$$

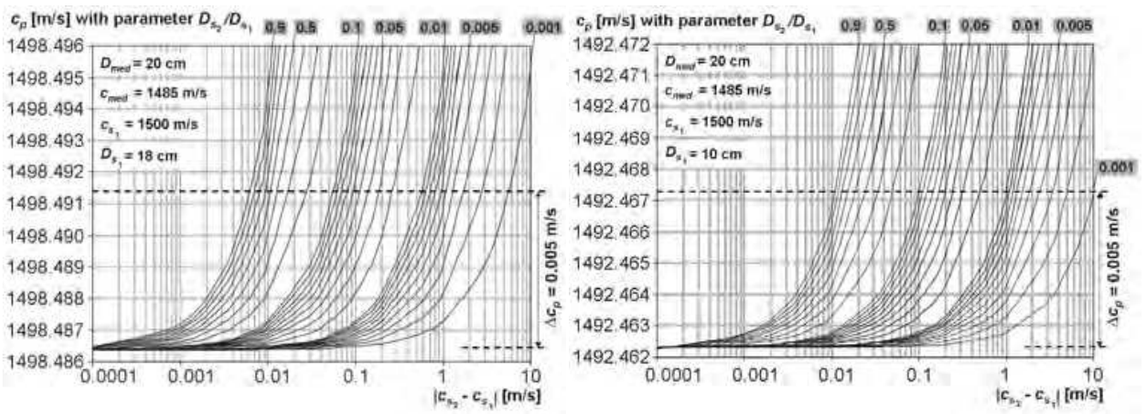


(a) (b)

Fig. 3. Dependence of $c_p$ on $|c_{s2} - c_{s1}|$ (for $c_{s2} > c_{s1}$) with parameter $D_{s2}/D_{s1}$ (formula (5)), for different ratios of $D_{s1}/D_{med}$ = 0.9 (a), 0.5 (b)

Figures 3a and 3b (for $c_{s2} > c_{s1}$) and Figures 4a and 4b (for $c_{s1} > c_{s2}$) present dependences between mean (projective) sound speed value, determined using formula (5) and the absolute value of the speed difference in heterogeneity and its spherical surrounding (Fig.2) for 29 various ratios of their diameters (0.001, 0.002, ..., 0.01, 0.02, ..., 0.1, 0.2, ..., 0.9) and for two relations between sphere diameter and distance between transducers (0.9 and 0.5) (Opielinski & Gudra, 2006).

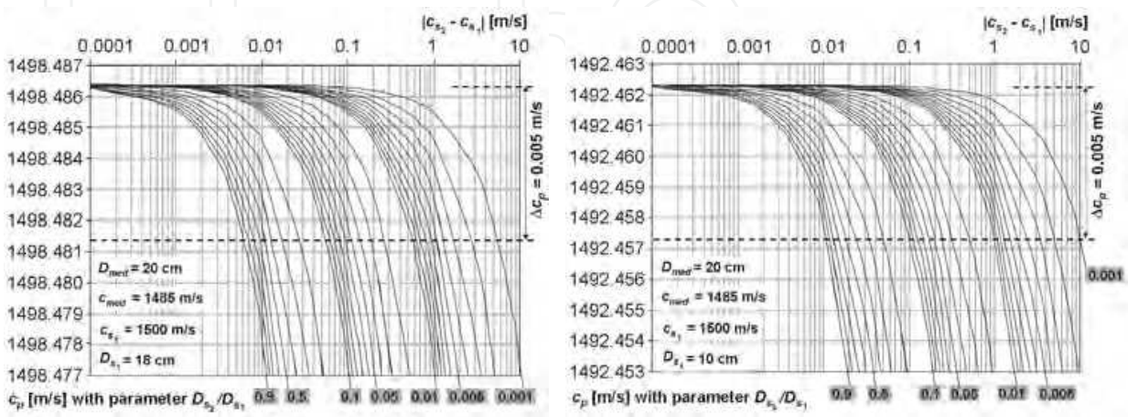


(a) (b)

Fig. 4. Dependence of $c_p$ on $|c_{s2} - c_{s1}|$ (for $c_{s1} > c_{s2}$) with parameter $D_{s2}/D_{s1}$ (formula (5)), for different ratios of $D_{s1}/D_{med}$ = 0.9 (a), 0.5 (b)

If we assume that the resolution of digital measurement of transition time at sampling frequency $f_s$, is $1/f_s$, then depending on the distance between surfaces of sending and receiving transducers and depending on the value of measured mean speed, the resolution of measurement of mean propagation speed of an ultrasonic wave (projection) can be determined using the formula (Fig.5) (Opielinski & Gudra, 2004b):

$$\Delta c_p = \frac{D_{med}}{D_{med} / c_p - 1 / f_s} - c_p \tag{6}$$

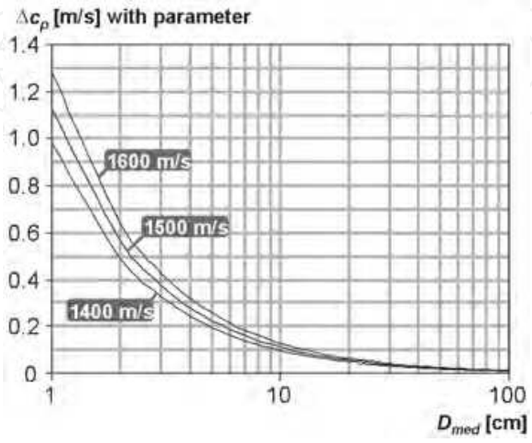


Fig. 5. Dependence of $\Delta c_p$ on $D_{med}$ (formula (6)) for different values of $c_p$ in a measurement area

For the diameter of measurement area $D_{med}$ = 20 cm, $f_s$ = 200 MHz ($T_s$ = 5 ns), $c_p$ = 1500 m/s, resolution $\Delta c_p \approx 0.06$ m/s. Using burst type ultrasonic pulses of the frequency of 5 MHz, 20 samples accrues to a half of wave period.

It means that at digital measuring of transition time, using the method of determining zero-crossing by the means of linear interpolation between samples of negative and positive amplitude values, it is possible to achieve the resolution of transition time measurement better than $\Delta t_p \approx T_p/2 = 2.5$ ns ($\Delta c_p \approx 0.03$ m/s); at a significant interval between a signal and noise (e.g. using algorithms of noise reduction), uncertainty of such measurements can be even better than about $\pm\Delta c_p/6 \approx \pm 0.005$ m/s (formula (6)).

Calculations show (Fig.3, Fig.4) that by the means of projection of ultrasonic wave propagation speed it is possible to detect differences of its local values in a biological structure. In case of a difference of speed in heterogeneity and its surrounding $|c_{s2} - c_{s1}| \approx 0$ (homogeneous sphere), all values of projection of speed $c_p$ tend to the determined value, marked by a dotted line in Fig.3a,b and Fig.4a,b. In order to conduct an interpretation of charts obtained from calculations, it is necessary to determine the resolution of measuring transition time of a wave through a structure. If we assume that using good class devices for digital measurements of transition time with interpolation it is possible to detect changes of sound speed of minimum about 0.005 m/s (dotted line in Fig.3a,b and Fig.4a,b) it can mean e.g. that for biological media of size of about 20 cm (in case of adjusting a distance between sending and receiving transducers to external dimensions of that media), by the means of ultrasound speed projection it is possible to detect heterogeneity of a local value of this speed in a structure (diversification) at the minimal level of about (Fig.3a):

a. 1 m/s for heterogeneity size $D_{s2} \approx 1$ mm,
b. 0.6 m/s for heterogeneity size $D_{s2} \approx 2$ mm,
c. 0.2 m/s for heterogeneity size $D_{s2} \approx 5$ mm,
d. 0.1 m/s for heterogeneity size $D_{s2} \approx 10$ mm,

considering that there still is an obligatory limitation due to the diffraction of an ultrasonic wave (a wave penetrates heterogeneities of sizes larger than a half of wave's length). Resolution of a detection of differences of local sound speed values in heterogeneity and its surrounding strongly depends on the ratio of their dimensions $D_{s2}/D_{s1}$ and the ratio of the size of an analysed object in the axis of ultrasonic transducers – sending and receiving – to the distance between the transducers $D_{s1}/D_{med}$ (the less ratios, the worse resolution – compare: Figures: 3a with 3b, and 4a with 4b).

A similar analysis was conducted for the projection of a frequency derivative of the ultrasonic wave amplitude attenuation coefficient, obtained after a transition of a wave through the model of a heterogeneous sphere in its axis (Fig.2). In case of projective measurements of the value of a frequency derivative of the amplitude attenuation coefficient of an ultrasonic wave by the means of detecting the frequency of a pulse of an ultrasonic wave after the transition, it is possible to assume a minimal uncertainty of the measurement of the projective value of frequency of about 2 kHz, what at assuming the ultrasonic wave frequency of 2 MHz, results in the uncertainty of determining the projective value of a frequency derivative of attenuation coefficient of about 0.001 dB/(cm·MHz). It means that in the measured projective values of receiving signal frequencies, it is possible to distinguish an influence of a heterogeneity for its dimensions proper correlated with a difference of a local value of the amplitude coefficient of attenuation of an ultrasonic wave in the structure of this heterogeneity and in the structure of

its surroundings $\Delta a$. If the presence of a heterogeneity changes measured projective values of a receiving pulse frequency, this heterogeneity is able to be detected. Calculations prove that at assuming the total uncertainty of projective measurements of values of the receiving pulse frequency of 2 kHz, it shall be possible to detect in a projective image heterogeneities, which differ from surrounding tissue by the minimum value of sound attenuation about: 0.1 dB/cm of the size > 9 mm, 0.2 dB/cm of the size > 4 mm, 0.5 dB/cm of the size > 2 mm, 1 dB/cm of the size > 900 μm, 2 dB/cm of the size > 400 μm, 5 dB/cm of the size > 200 μm. Calculated contrast resolution increases at higher spectrum width of the receiving pulse and a change of sound attenuation in water around a sphere has a negligible influence on this resolution.

In case of heterogeneities of diversified sizes, it can happen that in projective images for several projection planes, heterogeneities can be visible, while in others can be not.

## 5. Computer simulation of ultrasonic projection data

By the means of elaborated software, there was done a simulation of a distribution of local values of propagation velocity of an ultrasonic wave inside several three-dimensional objects immersed in water (Fig.6), and next, for a selected projection plane, there was done a calculation (using the Radon transform (Kak & Slaney, 1988)) of distributions of mean values (projections) in a parallel-ray geometry, at the set distance $D_{med}$ = 20 cm between surfaces of the transmitter and the receiver (Opielinski & Gudra, 2004c, 2006). In the space surrounding each of the objects, the speed of ultrasonic wave propagation was assumed at $c_{med}$ = 1485 m/s, what corresponds to the speed of sound in water of the temperature of about 21°C. In case of ultrasonic projection, using water as a coupling medium is obligatory due to a matching to the acoustic impedance of an examined biological structure. The Section 5 presents simulations of projective data for exemplary virtual objects *C* and *D*. Object *C* is a sphere of the diameter of 14 cm, containing 7 homogeneous balls of 0.5 cm diameters each, situated on the major axis, at 2 cm intervals between their centres, apart from two terminal ones - 1.85 cm intervals. Object *D* is an ellipsoid of the semi-major axis of 7 cm and the 1 cm semi-minor axis, containing 7 homogeneous balls of 0.5 cm diameters each, located on the diameter in the same way as in the object *C*. Local values of ultrasonic wave propagation speed are 1500 m/s for each point of the interior of objects *C* and *D*, apart from small balls – 1499 m/s.

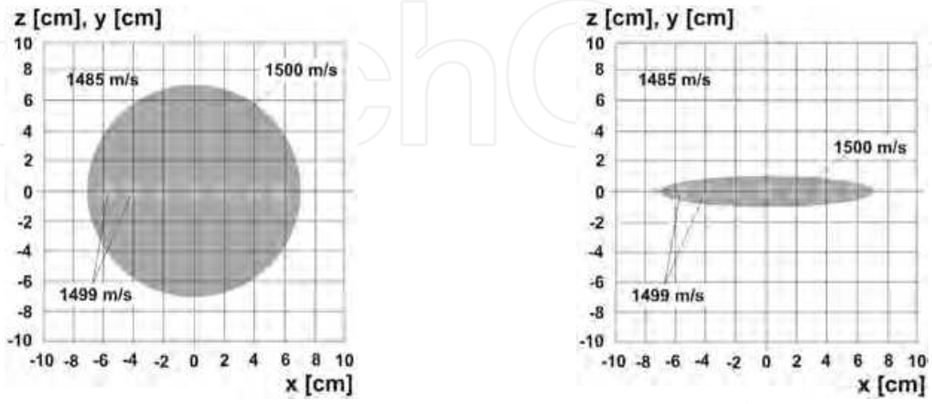


(a) (b)

Fig. 6. Shape of created 3-D virtual objects in cross-section: a) object *C* – small balls in sphere, b) object *D* – small balls in ellipsoid

Figure 7 presents images of ultrasonic projection for objects *C* and *D* obtained on the basis of computer simulated measurements of mean values of sound speed in an orthogonal projection (Opielinski & Gudra, 2004c). These values were linearly imaged in greyscale, from black to white. Shapes of projected objects, together with edges, are clearly visible in images. The object *C* interior seems to be homogeneous (Fig.7a) and spherical structures inside object *D* (Fig.7b) are hardly visible against the background of the ellipsoid projection (bright, round spots).

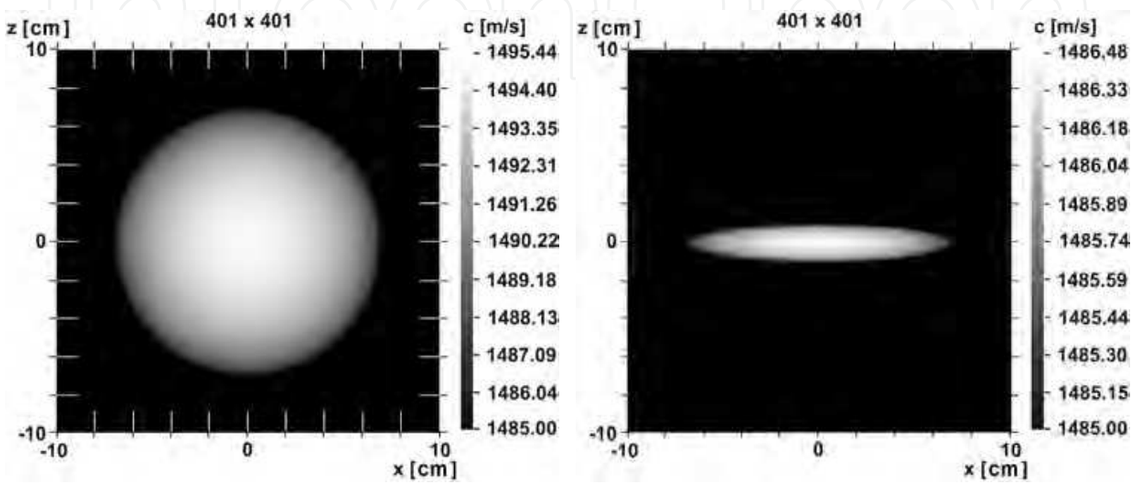


(a) (b)

Fig. 7. Ultrasonic projection images of objects shown in Fig.6, obtained on the basis of computer-simulated measurements of mean values of ultrasonic wave propagation velocity: a) object *C*, b) object *D*

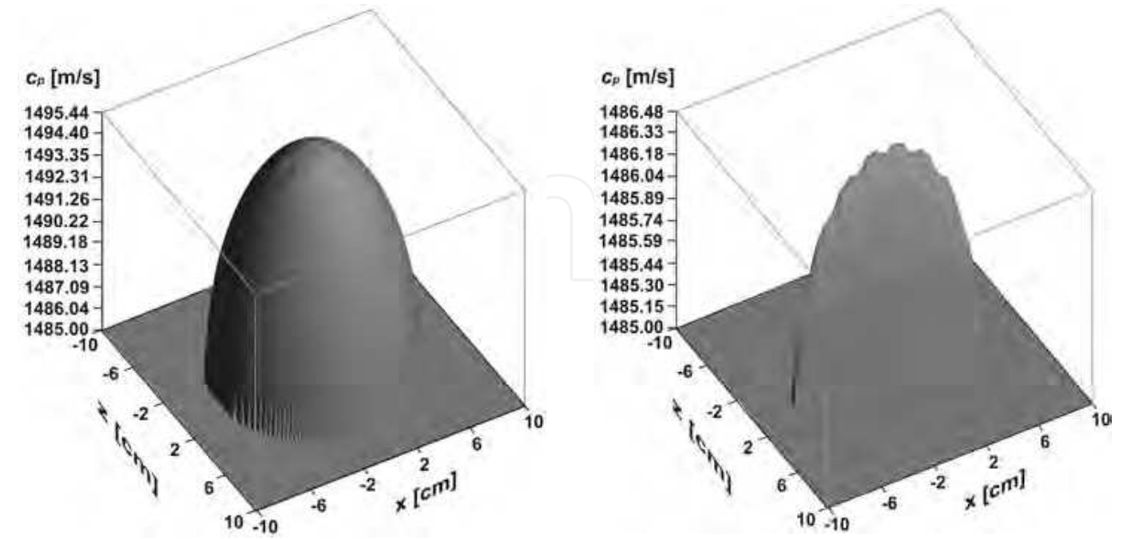


(a) (b)

Fig. 8. Ultrasonic projection images of sphere – object *C* (a) and ellipsoid – object *D* (b), shown in pseudo-3-D

In order to improve the contrast of visualisation of heterogeneous structures, Figure 8 presents ultrasonic projection images of objects *C* and *D* in pseudo-three-dimensional way with an lighting, imaging mean values of propagation speed of an ultrasonic wave for the plane parallel to the axis, along which small balls are arranged in the Cartesian co-ordinate system. Here, projections of spherical heterogeneities are shown in the form of characteristic oval concavities in the object's structure. Difficulties in imaging inclusions in the object *D* structure result from the projective method of averaging values of ultrasonic wave speed on the propagation path. In the projection images (Fig.7), objects' shapes and their edges are clearly visible in the parallel projection. Small spherical heterogeneities inside the sphere are hardly evident on the projective pseudo-three-dimensional image (Fig.8) due to scant sizes in comparison to the diameter of surrounding sphere.

Conducted simulative calculations enable an initial estimation of the accuracy of the ultrasonic projective imaging in respect of detecting heterogeneities in the internal structure. In the contour image of object *C* (Fig.7a), structure heterogeneities are imperceptible and in the contour image of object *D* (Fig.7b) – hardly visible. The reason of such imaging in ultrasonic projection is mainly a small difference of propagation velocity of an ultrasonic wave in heterogeneities in comparison to propagation in their surrounding (1 m/s). Projection values of sound velocity of propagation of an ultrasonic wave, corresponding to central pixels of the image from Figures 7a and 7b, are equal to 1495.4185 m/s and 1486.4374 m/s, respectively. If structures of objects *C* and *D* were homogeneous, these values would be equal to 1495.4683 m/s and 1486.4865 m/s, what means that an inclusion in the form of a central ball changes the velocity by about 0.05 m/s in both cases. Thus, such small change is not visible in contour images, due to a limited human eye's ability of distinguishing shades; however, it is noticeable in pseudo-3-D images (Fig.8). It seems that in ultrasonic projection it is possible to image even smaller differences in velocity values, thanks to using additional operations of data processing in the form of algorithms of compression, expansion, gating, filtration and limitation of measurement data values (Opielinski & Gudra, 2000).

The change of mean speed caused by an inclusion is approximately the same for objects *C* and *D*, however, their widths are significantly various. It means that a deterioration of the dynamics of velocity values simulated for object *C* is caused by too big distance between sending and receiving transducers – sound speed in the measurement medium (water) has a negative influence on measurement results. Due to the above, such distance should be possibly slightly higher from the size of an object in the analysed projection.

## 6. Projection measurements

The developed, computer-assisted measurement setup for examining biological structures by the means of ultrasonic projection, in the set of single-element ultrasonic probes - sending and receiving - is presented in Fig.9 (Opielinski & Gudra, 2004c, 2005).

For the aims of scanning of objects immersed in water, there were used two ultrasonic probes of 5 mm diameter, which played roles of a source and a detector of ultrasonic waves, of work frequency of 5 MHz (Opielinski & Gudra, 2005). Probes, mounted on the axis opposite each other, are shifted with a meander move with a set step in a selected plane of an object. Movements of probes are controlled by the means of a computer software through RS232 bus, using mechanisms of shifting *XYZ* (Opielinski & Gudra, 2005). The sending probe is supplied by a burst-type sinusoidal signal and pulses received from the receiving

probe by a digital oscilloscope are sent through RS232 bus to a computer and stored on a hard disk. Projective values of proper acoustic parameters, determined from particular receiving pulses, are imaged in the contour form in colour or grey scale and also in pseudo-3-D, using special software, which enables also advanced image processing (Opielinski & Gudra, 2005).

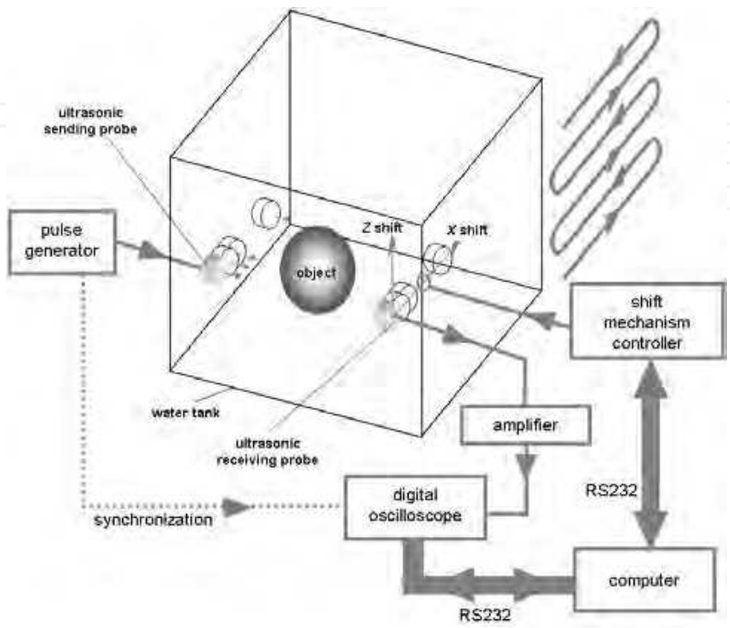


Fig. 9. Block scheme of the measurement setup for biological media structure imaging by means of the ultrasonic projection method using one-element ultrasonic probes

On the developed research setup, measurements of several 3-D biological objects were conducted in various scanning planes (Opielinski & Gudra, 2004b, 2004c, 2005, 2006). One of real biological media that was subjected to projective measurements was a hard-boiled chicken egg without a shell. Proteins composed of amino-acids are present in all living organisms, both animals and plants, and they are the most essential elements, being the basic structural material of tissues. A chicken egg is an easy accessible bio-molecular sample for ultrasonic examinations. Due to its oval shape (a possibility to transmit ultrasonic waves from numerous directions around it), structure and acoustic parameters (a relatively low attenuation and a slight refraction of beam rays of an ultrasonic waves at boundaries water/white/yolk), a boiled chicken egg without a shell is a great object, enabling testing of visualisation of biological structures by the means of ultrasonic projection and the method of ultrasonic transmission tomography (Opielinski, 2007). Figure 10 presents obtained projective images (the transmission method, $f$ = 5 MHz) in comparison to an image obtained from an ultrasonography (the reflection method, $f$ = 3.5 MHz) of a hard-boiled chicken egg without a shell. On the basis of the set of recorded receiving pulses in one scanning plane, with the step of 1.5 mm x 1.5 mm, images presenting the projection of a distribution of three various acoustic parameters in the object structure were obtained: propagation velocity, frequency derivative of ultrasonic waves attenuation and ultrasonic wave amplitude after transition (Opielinski & Gudra, 2004b, 2004c, 2005). In the images, distributions of particular parameters are marked by a solid line for pixels along marked broken lines. Negative values of a derivative of the ultrasonic wave attenuation on frequency in the image in Fig.10b result

from errors of the measurement of a shift of mid-frequency of pulse after transition at edges of structures, where a signal is weakened or faded most often.

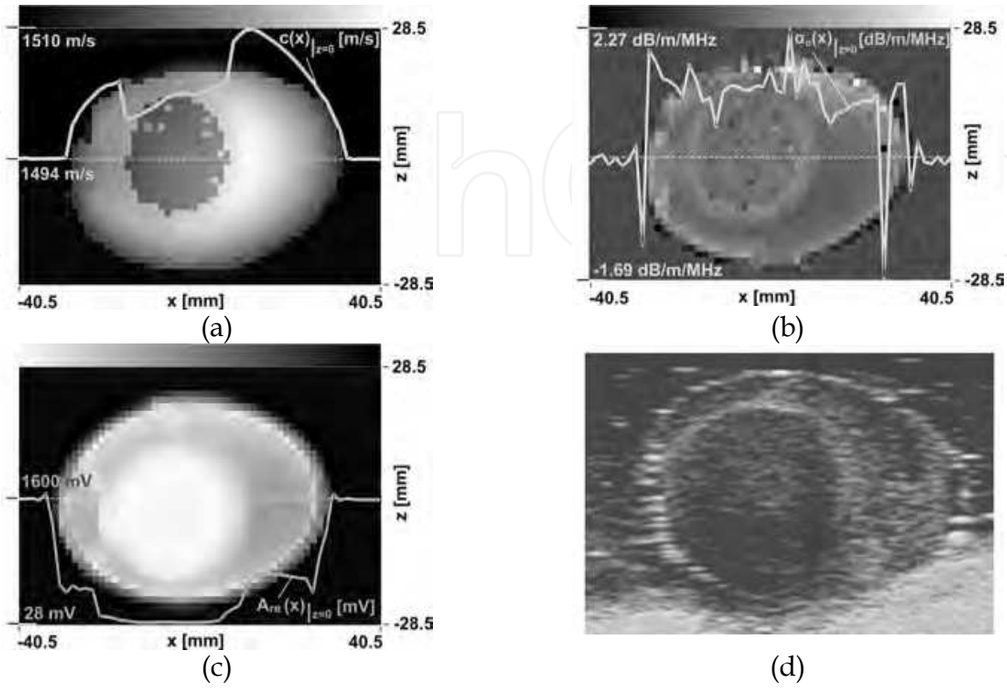


Fig. 10. Ultrasonic projection images of a hard-boiled hen's egg without shell, obtained from the following measurements of mean values: a) ultrasonic wave propagation velocity, b) derivative of the ultrasonic wave amplitude attenuation coefficient on frequency, c) ultrasonic wave pulse amplitude, in comparison to the ultrasonogram of the same egg (d)

In order to verify the correctness of imaging the internal structure of the analysed object, Fig.11 presents its optical image in the cross-section for the analysed plane, obtained after cutting an egg into half and scanning the examined section using an optical scanner. Comparing images presented in Figures 10 and 11, it can be unequivocally stated that a computer-assisted ultrasonic projection enables proper recognising of biological structures (a yolk is clearly visible in the egg structure). One advantage of the ultrasonic projection method is an availability to obtain several different images from a single measurement set, every of which characterises some other features of an object.

Fig. 11. The optical image (scan) of the measured egg cross-section structure

These images can be properly processed and correlated by the means of special software, what enables recognising structures, which are not visible in single images. The image of the distribution of the sound speed projection values clearly visualises constant changes of heterogeneity (Fig.10a), while the image of the distribution of sound attenuation frequency derivative projection values better visualises discrete changes (Fig.10b). In the image of the distribution of sound velocity projection values, it is also visible that sound speed in a yolk is higher than in water and lower than in white of an egg (Fig.10a). In the image of the distribution of the amplitude projection values, it is visible that attenuation in yolk is larger than in egg white and much higher than in water. The image of the distribution of amplitudes of receiving pulses is characterized by a large dynamics of value changes and in a similar rate visualises both continuous and step changes (Fig.10c). The ultrasonographic image of an egg (Fig.10d) visualises clearly only boundaries of yolk and white structures.

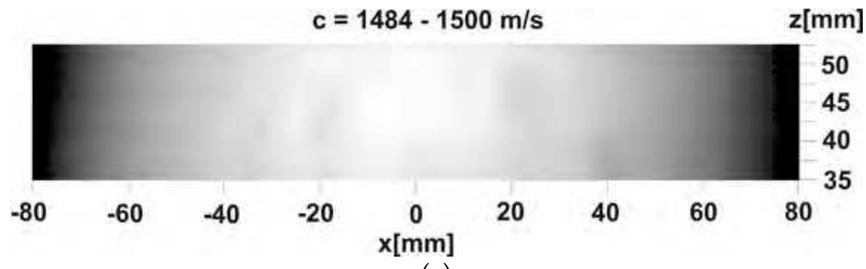


(a)

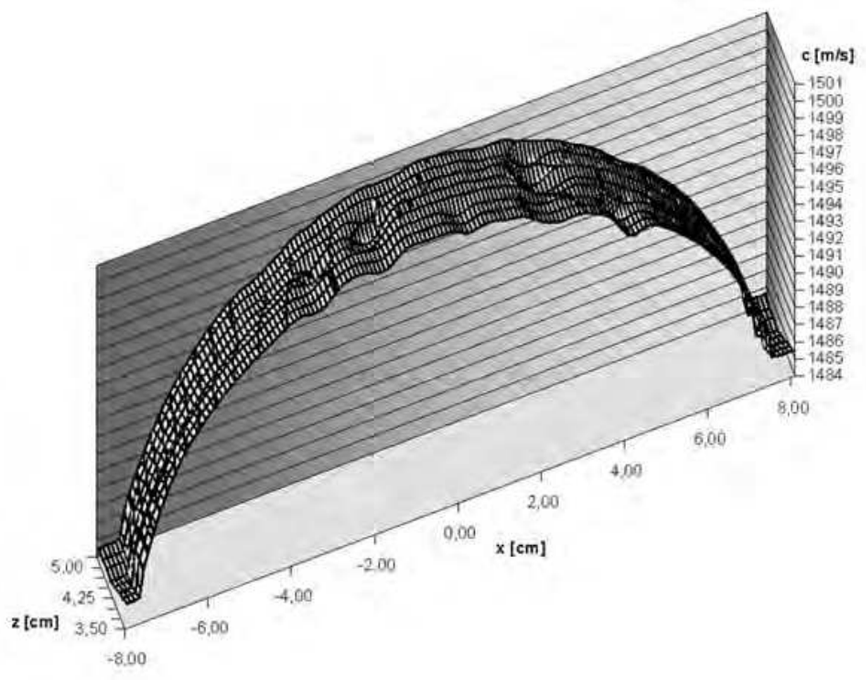


(b)

Fig. 12. Ultrasonic projection images of CIRS model 052 breast biopsy phantom in the range of measured altitudes $h$ = 3.50 ÷ 5.25 mm along its longest dimension – length: a) image in gray scale, b) image in pseudo-3-D

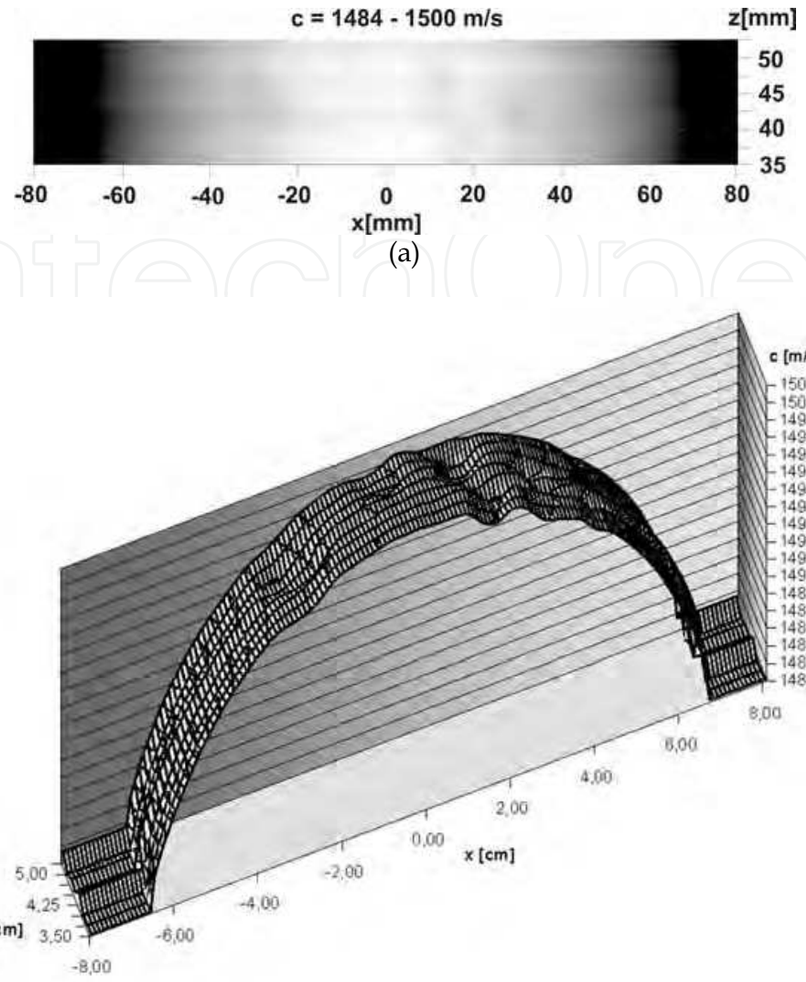


Fig. 13. Ultrasonic projection images of CIRS model 052 breast biopsy phantom in the range of measured altitudes $h$ = 3.50 ÷ 5.25 mm, along its shortest dimension – width: a) image in gray scale, b) image in pseudo-3-D

A subject of projection studies was also a breast biopsy phantom of the American CIRS company, model 052, which simulates acoustic parameters of tissues that are present in a female breast. Ultrasonic projection measurements of the CIRS phantom were conducted on the research setup for ultrasonic transmission tomography (Opielinski & Gudra, 2010b), measuring mean values of transition times of an ultrasonic pulse in the geometry of parallel-ray projections, by the means of single-element ultrasonic probes of 5 mm diameters and work frequency of 5 MHz, located centrally opposite each other, in the distance of 160 mm (Opielinski & Gudra, 2004a, 2004c). There were used 161 steps of probes pair shift along the phantom, with the 1 mm step (161 measurement rays) for each of 100 turns around the phantom with the step of 1.8° (100 measurement projections) and for each of eight positions of probes pair in vertical direction, in distances from the phantom base of 35 mm, 37.5 mm, 40 mm, 42.5 mm, 45 mm, 47.5 mm 50 mm, 52.5 mm, respectively. Such data set enables

obtaining 100 projection images in *XZ* planes (of resolutions 101 x 8 pixels each), from all sides of the object flank, in the angle range of 0° ÷ 178.2°. Figures 12 and 13 present images of sound speed projections for parallel ultrasonic rays, penetrating lateral surfaces of the CIRS phantom in the range of measured heights of $h$ = 3.50 ÷ 5.25 mm, in greyscale and pseudo-3-D (Opielinski & Gudra, 2004c).

These images were obtained by temperature scaling and assembling all measurement projections (sets of values for full shifts of the probes pair along the object) for rotation angles of 0° (Fig.12) and 90° (Fig.13), extracted from projection measurement sets of cross-sections of the phantom for particular heights.

Figure 14 presents 2 geometrical projections of the CIRS breast phantom structure from the sides of its length and width, obtained by the means of 3-D reconstruction from tomographic images (Opielinski & Gudra, 2004a, 2004c). It can be observed that there is a good conformity of geometrical projections of the phantom with projection images obtained by the means of ultrasound transmission (compare Fig.12 and Fig.13 with Fig.14a,b). An interpretation of projection images requires a spatial intelligence and basic knowledge in spatial geometry. Particular images present projections of the distribution of local values of a measured acoustic parameter in the plane parallel to the scan surface and are a mirror reflection for projection planes from the back and front sides of the object. Projection imaging is not a full quantitative imaging; however, on the basis of values of particular pixels of an image it is possible to determine the diversification of parameters of an examined structure. At a proper resolution, step changes of values of an examined acoustic parameter in the projection plane are noticeable in an image, while continuous changes are, in general, not easy detectable. A step change of values of an examined parameter is visible in a contour image in the form of a discrete change of contrast. Pseudo-3-D images provide a better dynamics of projection visualisation. On the basis of several projection images of an examined structure from numerous directions, it is possible to undertake an attempt of a 3-D reconstruction of heterogeneity borders in its interior (Opielinski & Gudra, 2004a).

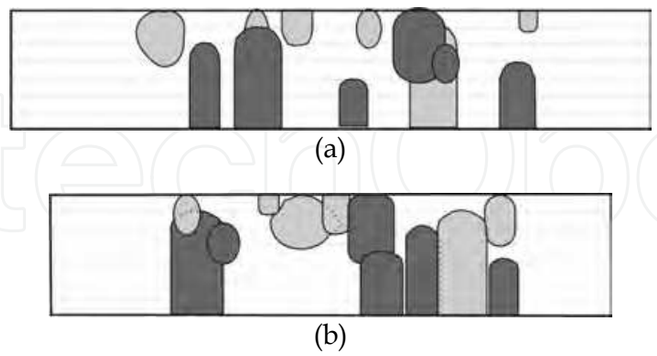

(a)

(b)

Fig. 14. Geometric projections of phantom CIRS structure along its length (a) and width (b), obtained on the basis of three-dimensional reconstruction from tomographic images

Ultrasonic projection imaging can be also used for non-invasive *in vivo* visualisation of injuries and lesions of human upper and lower limbs (Ermert et al., 2000) for the aims of e.g. diagnosing osteoporosis degree. However, it is necessary to consider specific distortions, which occur in an image due to refraction of ultrasonic wave rays in case of biological

structures of a large refraction index (the ratio of velocity in water to velocity in an examined structure (Opielinski & Gudra, 2008)). In case of bones examinations, it is possible not only to record projection values of acoustic parameters described in Section 3, but also to determine images of the distribution o two main parameters of ultrasonic waves, used in medicine for diagnosing various stages of osteoporosis: SOS (speed of sound) and BUA (broadband ultrasound attenuation). On their basis, it is also to determine the distribution of the stiffness factor, which defines the state of osseous tissues in relation to a healthy female population, in the age of so called peak bone mass.

## 7. 2-D ultrasonic matrices

At designing multi-element ultrasonic matrices – sending and receiving one – for the aims of projective imaging of biological media, it is essential to achieve a compromise between the resolution (it depends on the type and size of elementary transducers, their work frequency, distance between them) and the efficiency and sensitivity, which grows along with the surface size of an elementary transducer. Thus, it is very important to specify the sizes of elementary transducers and distances between them already at the designing stage. The technique of mounting transducers on a matrix and the way of conducting electrodes has also a substantial influence on the way of transducers' work. The ongoing search for improved ultrasonic imaging performance will continue to introduce new challenges for beamforming design (Thomenius, 1996). The goal of beamformer is to create as narrow and uniform a beam with as low sidelobes over as long a depth as possible. Among already proposed imaging methods and techniques are elevation focusing (1.25-D, 1.5-D and 1.75-D arrays) (Wildes et al., 1997), beam steering, synthetic apertures, 2-D and sparse matrices, configurable matrices, parallel beamforming, micro-beamformers, rectilinear scanning, coded excitation, phased subarray processing, phase aberration correction, and others (Drinkwater & Wilcox, 2006; Johnson et al., 2005; Karaman et al., 2009; Kim & Song, 2006; Lockwood & Foster, 1996; Nowicki et al., 2009). The most common complication introduced by these is a significant increase in channel count. Generating narrow ultrasonic wave beams in biological media by multi-element probes, built as matrices of elementary piezoceramic transducers in a rectangular configuration, can be realised using transducers having a spherical surface, ultrasonic lenses, mechanical elements (e.g. complex system of properly rotated prisms), focusing devices or electronic devices, which control the system of activating and powering individual matrix elements in a proper manner (Drinkwater & Wilcox, 2006; Ermert et al., 2000; Granz & Oppelt, 1987; Green et al., 1974; Nowicki, 1995; Opielinski et al., 2009; Opielinski & Gudra, 2010a, 2010c; Opielinski et al. 2010a, 2010b; Ramm & Smith, 1983; Thomenius, 1996). Exciting individual transducers of the multi-element probe using pulses with various delay is a universal method of focusing and deflecting a beam (Johnson et al., 2005; Thomenius, 1996). Adequate delays between activations of each successive elementary transducer allow shaping of the wave front and the direction of its propagation. In case of multi-element ultrasonic matrices (Opielinski et al., 2009, 2010a, 2010b) used for projection imaging of internal structure of biological media (Ermert et al., 2000; Granz & Oppelt, 1987; Green et al., 1974; Opielinski & Gudra, 2005), introduction of delays of propagation of pulse ultrasonic wave for individual transducers can result in

imaging errors associated with side lobes. However there are a number of mechanisms that suppress grating side lobes (a few wavelengths short excitation pulses, apodization weighting functions, a different transmit and receive geometries, random element spacing) and hence allow this criterion to be somewhat relaxed in practice (Drinkwater & Wilcox, 2006; Karaman et al., 2009; Kim & Song, 2006; Lockwood & Foster, 1996; Thomenius, 1996; Yen & Smith, 2004). This method of focusing makes it also necessary to develop synchronised delaying systems and sophisticated technologies of attaching a large number of electrodes to the surface of minute piezoceramic transducers by integration of some of the electronics with the transducer matrix enabling for miniaturization of the front-end and funnelling the electrical connections of a 2-D matrix consisted with hundreds of elements into reduced number of channels (Eames & Hossack, 2008; Opielinski et al., 2010a, 2010b; Wygant et al., 2006a; 2006b; Yen, Smith, 2004).

The experimental results have shown that using double ultrasonic pulse transmission of short coded sequences based on well-known Golay complementary codes allows considerably suppressing the noise level (Drinkwater & Wilcox, 2006). However this type of transmission is more time consuming.

Increase of directivity and intensity of the wave generated by the multi-element ultrasonic probe can be achieved by simultaneous in phase powering (no delays) of sequences of many elementary transducers (using one generator) in the sending system (which will however result in the probe's input impedance decrease) or by simultaneous receiving ultrasonic wave by means of sequences of many elementary transducers (Chiao & Thomas, 1996; Hoctor & Kassam, 1990; Karaman et al., 2009; Lockwood & Foster, 1996; Opielinski & Gudra, 2010c; Wygant et al., 2006a; Yen & Smith, 2004). Such sending probes are usually activated by low power generators of sinusoidal burst type pulses, the generated voltage values of which are low (a couple of tens of volts peak-to-peak) and output resistance of about 50 Ω. If the probe's impedance is close to output impedance of the generator, it results in a decrease of amplitude of activating pulse voltage which in turn causes decrease of intensity of the ultrasonic wave generated in the medium.

Recently in the medical imaging field a number of authors have suggested the use of matrices with large numbers of elements and investigated methods of selecting the optimal numbers and distribution of elements for the transmit and receive apertures (Drinkwater & Wilcox, 2006). The development of 2-D matrices for clinical ultrasound imaging could greatly improve the detection of small or low contrast structures. Using 2-D matrices, the ultrasound beam could be symmetrically focused and scanned throughout a volume (Lockwood & Foster, 1996; Yen & Smith, 2004).

This Section (7) presents an idea of minimising the number of connections between individual piezoelectric transducers in a row-column multi-element ultrasonic matrix system used for imaging of biological media structure by means of ultrasonic projection (Opielinski & Gudra, 2010c; Opielinski et al., 2010a, 2010b). It allows achieving significant directivity and increased wave intensity with acceptable matrix input impedance decrease without any complicated and expensive focusing or 2-D beamforming systems, what is a great advantage. This concept results in the necessity of creating several small models (e.g. square matrices of 16 transducers in 4 x 4 configuration) at the designing stage, in order to

optimally select all essential parameters, together with developing a proper production technology (Opielinski & Gudra, 2010a). Such technology can be easily copied later with proper modifications and improvements, developing the matrix model by adding a greater number of elementary transducers. The following assumptions of constructing multi-element ultrasonic matrices were adopted (Opielinski & Gudra, 2010a):

a. transducer work frequency in a biological medium in the range of $f_r$ = 1 MHz ÷ 2 MHz, in order to achieve a proper depth resolution (measurement accuracy) and relatively low attenuation of an ultrasonic wave,
b. dimensions of matrix piezoceramic transducers of $a \approx 1.5$ mm, $b \approx 1.5$ mm, in order to achieve a proper scanning resolution, identical all over matrix plane,
c. distance between transducers of $d \approx 1$ mm, in order to enable conducting electrodes and mounting matrices in laboratory conditions.

Desired dimensions of elementary piezoceramic transducers at possibly least material losses were achieved thanks to mechanical cutting with a diamond saw of 0.2 mm thickness. Cut plates were selected from a larger group due to repeatability of work frequency and electric conductance values.

### 7.1 Ultrasonic standard matrices

First of all, ultrasonic 512-element standard matrices (with separated electrodes connections) assigned for work in the sending and receiving character were constructed from SONOX P2 piezoceramic transducers, of the size of 1.5 x 1.5 mm (Opielinski & Gudra, 2010a). For a precise mounting of transducers, a mask made of engraving laminate of 0.8 mm thickness, with square-shaped holes for elementary transducers, cut using laser, at accuracy of 10 μm was used. At the back side (ground), transducers were stuck using conducting glue, to properly etched paths of a printed-circuit board, located at distances of 1 mm each other, in the layout of 16 rows and 32 columns. In order to connect a signal lead (electrode) to the active surface of each elementary transducer of the matrix, contact elastic connection was used. The lead, bent in the form of a hook, elastically adhering to the transducer surface, is conducted to the other side through the hole in the printed-circuit board, where it is stuck to its surface. The matching layer of matrices, which also serves the roles of isolation and stabilisation of contacts, was made by spraying a proper lacquer over their surfaces. A picture of the developed standard ultrasonic matrix is shown in Fig.15 (Opielinski & Gudra, 2010a). Detailed measurements of electro-mechanical parameters of elementary ultrasonic transducers of the developed standard matrix showed a presence of three resonance frequencies $f_{r1} \approx 1$ MHz, $f_{r2} \approx 1.8$ MHz and $f_{r3} \approx 2$ MHz. The reasons of occurrence of so many resonances is the assumed way of mounting transducers using conducting glue to proper patch of the board, without a back attenuation layer. The average efficiency of elementary transducers of the standard matrix, in the distance of 2.5 cm from the surface can be estimated on average at about 750 Pa/V for $fr_1$ = 1.1 MHz and at about 400 Pa/V for $fr_2$ = 2.1 MHz. Study results show that the developed standard matrices are suitable for projective imaging of biological media of parameters close to parameters of soft tissues, using the scanning method through switching proper pairs of sending and receiving elementary transducers (or proper synthetic apertures (Opielinski & Gudra, 2010c)).

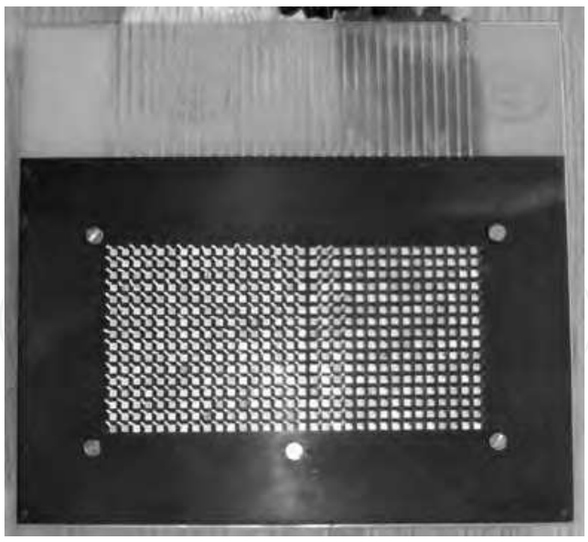

Fig. 15. Photo of the developed 512-element standard matrix for ultrasonic projection examinations

### 7.2 Ultrasonic passive matrices

An increase of directivity and intensity of the wave generated by the multi-element standard 2-D ultrasonic matrix (Section 7.1) can be obtained by simultaneous in phase supply (without delays) of a sequence of numerous elementary transducers, using one generator in the transmitting set-up (an aperture in transmitting and/or in receiving set-up - (Opielinski & Gudra, 2010c)), what causes a drop of the input impedance of the matrix. Such matrices are, usually, powered by low-power generators of burst-type sinusoidal pulses of low values of generated voltages (max. 20 $V_{pp}$) and output resistance of about 50 Ω. If the matrix sending transducer group impedance is close to the output impedance of the generator, a drop of the amplitude of an exciting pulse voltage occurs, what is followed by a drop of the intensity of the ultrasonic wave, which is generated to a medium. In the far field, in the plane perpendicular to axis $Z$, a distribution of the acoustic field generated by multi-element matrices with simultaneous supply to the group of elementary transducers has consecutive maxima and minima. Locations of maxima and minima and the acoustic pressure amplitude of the major and side lobes depend on the sizes of matrix's elementary transducers, distance between them and the length of the wave radiated into the medium. If the distance between adjacent transducers is small enough ($d < \lambda/2$), there are no side lobes in the area of 90°. This criterion is very difficult to be achieved as for the frequency of 2 MHz, the length of a wave in tissue is about 0.75 mm, what forces the use of elementary transducers of sizes below 0.375 mm. So, this Section (7.2) presents the concept of minimising the number of connections of particular piezoelectric transducers in the row-column arrangement of the multi-element ultrasonic passive matrix, assigned for imaging of biological media structures, by the means of the ultrasonic projection method (Opielinski et al., 2010a), what simultaneously enables achieving a large directivity and an increase of the wave intensity at acceptable drop of input impedance of the matrix.

So called passive matrix is the simplest solution for the matrix type controlling. This matrix includes two sets of keys (electronic switches), of which one $K_y$ selects an active column and

the second $W_x$ – an active row. In this way, transducer $P_{xy}$ is activated, which is located on the cross-cut of the selected row and column (Fig.16a). Piezoceramic transducers of the matrix are supplied with an alternating signal of high frequency (several MHz). Their structure (dielectric with sublimated electrodes) makes that, from the electronic circuit point of view, they have the capacitive character and an exciting signal can pass through inactive transducers to other rows and columns, despite disconnection of keys (Fig.16b). Directivity and efficiency/sensitivity of such matrix shall, therefore, depend to a high degree on a distribution of voltages of an exciting/receiving signal on all elementary transducers of the matrix, which in such way (with crosstalk) shall be excited to oscillations (Opielinski et al., 2010a).

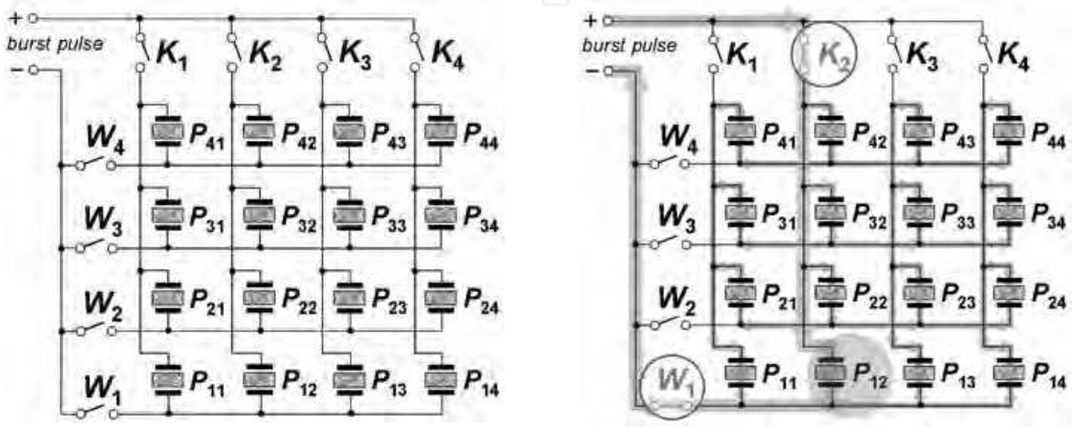


Fig. 16. Diagram of connections of transducers in a passive matrix (a) and a phenomenon of crosstalk formation (b)

Calculations and measurements of distributions of an acoustic field of the developed model of the 16-element passive matrix, in the 4 x 4 transducers layout, showed that after making a switch of one elementary transducer, all matrix transducers are excited by voltages, according to a specified pattern, thanks to which the matrix generated a directional beam. Exciting elementary transducers in a row-columns arrangement in a multi-element ultrasonic passive matrix enables a substantial minimisation of the number of connections of particular piezoelectric transducers. For example, for a 1024-element matrix, it is enough to use 64 paths, etched at a printed-circuit board, which conduct a signal exciting elementary transducers, instead of soldering 1024 separate electrodes in the form of thin, isolated leads to transducers surface and mounting multi-pin slots. The concept of a passive matrix enables also achieving a large directivity and an increase the wave intensity at an acceptable drop of the input impedance of the matrix. The developed concept of a passive matrix enabled designing of a full-sized matrix of 512 transducers, arranged in the structure of 16 rows and 32 columns. Due to a compact construction of the system, it was decided to put transducers and all electronic systems on a one printed circuit. Elements were arranged on the board with a division into two areas. The lower part is the proper matrix of transducers and the upper one includes switching circuits. Such strict division enables immersing the lower part in water, without the risk of damaging electronic circuits. Printed circuits include connections only for columns of the passive matrix. Connections of rows were realised using an additional upper board (microwave teflon-ceramic laminate) with a printed circuit,

which is simultaneously a mask for positioning transducers. It is a single-sided circuit, composed of sixteen especially designed horizontal paths. Each path has square areas deprived of copper. These areas mark locations of ultrasonic transducers and were cut out by the means of a special punch. Such square openings enable a precise placing of transducers. Electrical connection of ultrasonic transducers with the back base board were realised by hot-air soldering. The upper board (mask) thickness of about 0.8 mm was selected in order to locate transducer surface evenly with the board surface. A small amount of conducting glue enabled connection of transducer metallization with the path around a hole. There were developed two 512-element passive matrices with Pz37 Ferroperm ceramic transducers of the size 1.6 x 1.6 mm, arranged at the distances of 0.9 mm. One matrix is assigned for sending work and the second for receiving. Figure 17 presents the view of the developed 512-element ultrasonic passive matrix. Large round holes at the sides of matrix surface are designed for mounting semi-conducting lasers in the sending matrix for positioning the sending matrix with the receiving one.

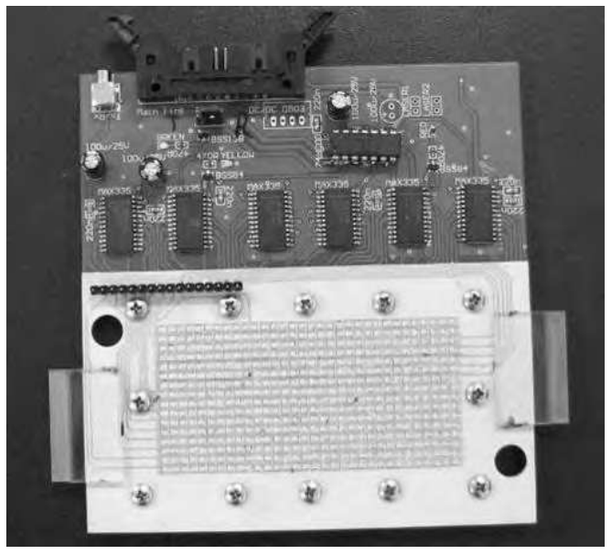

Fig. 17. The view of the developed 512-element ultrasonic passive matrix

One characteristic feature of the passive matrix is occurrence of crosstalk (Opielinski et al., 2010a), which causes a presence of some signal voltage, even on inactive transducers. This voltage is most often substantially lower than the voltage on a switched transducer but has an influence of the shape of obtained resultant characteristics of the matrix directivity. On the basis of conducted simulations and calculations, the following formula that describes the distribution of an excitement voltage on the passive 512-element matrix in the arrangement of $N$ x $M$ transducers was derived:

$$x = \frac{1}{(M-1)+(N-1)+1} \tag{7}$$

The switched on transducer of the passive matrix is supplied by voltage $+U$, all transducers in this (switched on) row are supplied by voltage $+U \cdot x \cdot (N-1)$, all transducers in this (switched on) column are supplied by $+U \cdot x \cdot (M-1)$, and all the other transducers (in switched

off rows and columns) are supplied by voltage $-U \cdot x$. The simulated in this way distribution of voltages for the passive matrix of 16 x 32 sizes is presented in Fig.18. Elementary transducers of the passive matrix, in the frequency range of 1.4 ÷ 2.4 MHz, exhibit a possibility of working at three resonance frequencies $f_{r1} \approx 1.6$ MHz, $f_{r2} \approx 1.8$ MHz, $f_{r3} \approx 2$ MHz. The imaginary part of the amplitude-phase electrical admittance characteristics of transducers of the passive matrix reveals their capacitive character ($C_o \approx 160$ pF, including the capacity of connection leads of about 100 pF, $R_o \approx 3$ kΩ $|Z(f_r)| \approx 2$ kΩ).

| | | |
|---|---|---|
| -0.021 | 0.66 | -0.021 |
| 0.32 | 1 | 0.32 |
| -0.021 | 0.66 | -0.021 |

Fig. 18. Simulated distribution of values of voltages exciting elementary transducers of the passive matrix of 16 x 32 transducers arrangement („–" marks a inversed phase)

Single transducers of the earlier developed multi-element matrices with separated electrode connections (standard matrices) exhibited electrical capacity $C_o \approx 10$ pF, resistance of electric losses $R_o \approx 30$ kΩ and electric impedance in resonance $|Z(f_r)| \approx 7$ kΩ (Opielinski & Gudra, 2010a) (for a comparison, at simultaneously excitement of 16 transducers of the standard matrix with the same voltage $U$, impedance of the circuit would be $|Z(f_r)| \approx 440$ Ω). These values suggest that in case of the passive matrix, the phenomenon of increasing electric capacity of transducers and reducing their losses resistance occurs due to a parallel connection of all matrix elements, what is confirmed by the presence of crosstalk in such arrangement. Measurements and calculations show that the developed passive matrix enable achieving much larger directivity and almost three time higher amplitude of an ultrasonic wave generated in a medium than in case of a single supply, electrically separated transducer of the standard matrix (Opielinski & Gudra, 2010a). The divergence angle of the beam generated by the developed 16-element model of a passive matrix in the 4 x 4 arrangement, with an activation of 1 element is about 6 ÷ 8°.

### 7.3 Ultrasonic active matrices

A large number of elementary transducer of a projection matrix forces a high number of electrical connections and substantially makes miniaturisation of the whole unit difficult. A solution to such inconvenience is using a row-column selection of active transducers (so called passive matrix), presented in Section 7.2. For the matrix of 512 elements, arranged in 16 rows and 32 columns, it is enough to connect 48 leads (16+32) this way, instead of 512. A solution that can enable elimination of crosstalk between transducers in the passive matrix (Fig.16) with the maintenance of the electrode minimisation is the use of active elements (keys) in matrix nodes (active matrix) (Opielinski et al., 2010b). In this solution, each transducer is switched by its own individual key $T_{xy}$ (Fig.19).

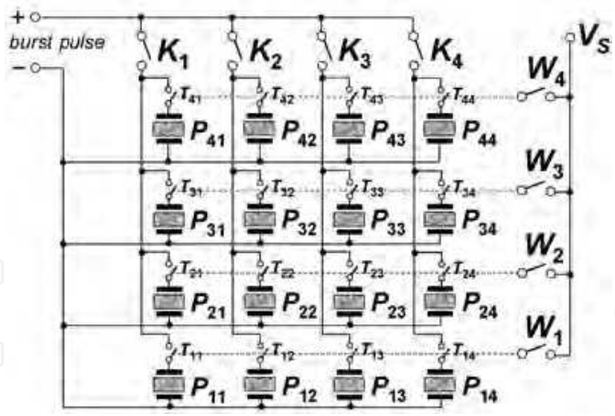


Fig. 19. Diagram of transducer connections in an active matrix

Key $K_y$ in the signal path conducts voltage to a particular column, while a closing of keys $W_x$ determines an activated row. Field-effect transistors play the role of individual keys $T_{xy}$. Their advantage is a small housing size, what enables a miniaturisation of connections.

On the basis of earlier conducted experiment, similarly as in case of the passive matrix, an active matrix, including 512 ultrasonic transducers was developed. Its construction assumes the use of two keys switching signal on for each of elementary transducer. Such solution complicates the matrix construction but enables elimination of crosstalk, present in the passive matrix. Matrix control is realised in a similar way as in the passive matrix (section 7.2), however, circuits of switching matrix columns were more developed. Only an active column is connected to the signal source and all other are shorted to ground. It eliminates a possibility of signal slips into inactive columns. Thanks to utilisation of individual transistors at each piezoceramic transducer, there is no need to key signal in matrix rows (Fig.20). This way, using additional keys $K_{zy}$ (Fig.20), the active matrix is working as a standard matrix (see Section 7.1). Without using additional keys $K_{zy}$ (Fig.20), after switching electrodes to a proper row (key $W_x$) and column (key $K_y$) of the matrix and after switching a transistor key for a certain transducer (key $T_{xy}$) (see Fig.19), it shall be excited by fed voltage $U$, and other transducers in this column shall be excited with a voltage below $0.3 \cdot U$ (Opielinski et al., 2010b).


Fig. 20. The method of crosstalk elimination in a column of the active matrix using additional switches $K_{zy}$: (a) short-circuiting an inactive transducer, (b) open-circuiting when activating a transducer

Application of such sending and receiving matrix in a projection arrangement is possible in such way that one of them is switched by the angle of 90º in relation to the other one and sequences of switching sending and receiving transducers are so coupled that enables a proper control of scanning of a received beam (Opielinski & Gudra, 2010b).

Active matrices act similarly as earlier developed standard matrices (Section 7.1) but their construction is more simple and improved.

## 8. Models of ultrasonic transmission camera

Using especially developed multi-element ultrasonic projection matrices with quick electronic switching of elementary transducers (Section 7), it is possible to obtain images in pseudo-real time (e.g. with a slight constant delay, resulting from the need of data buffering and processing), thus, a device using this method can be called an ultrasonic transmission camera (UTC) (Ermert et al., 2000). There are several know works regarding such cameras, conducted at some centres in the world, as described in Introduction (Brettel et al., 1981; Ermert et al., 2000; Granz & Oppelt, 1987; Green et al., 1974; Lehmann et al., 1999).

In the device presented in the work (Green et al., 1974), an incoherent ultrasonic wave was used for sonification of an object and a one-dimensional linear array, mounted in a set position served the role of a receiver. Scanning of an object structure in the second dimension was realised by the means of a complex system of properly rotated prisms. A disadvantage of such system is the necessity to use mechanical elements.

The device presented in (Brettel et al., 1981) uses a similar concept as in work (Green et al., 1974). The difference consists in the fact that a projection image is projected on the water surface of a camera and next, it is detected by a linear array of transducers. What is more, scanning in the second dimension was realised using mechanical movements of an array, instead of rotating prisms. A disadvantage of such system is the necessity to use mechanical elements.

The device presented in work (Granz & Oppelt, 1987) functions in pseudo-real time and its construction is similar to the camera described in (Brettel et al., 1981). An incoherent ultrasonic wave passes through an object in a wide beam in order to reduce the effect of spots. An image is obtained using a spherical mirror, located behind an object and in front of a 2-D, electronically controlled receiving matrix of PVDF foil transducers, in the arrangement of 128 x 128 elements. The camera enables obtaining images in pseudo-real time (with data buffering) at the rate of 25 frames per second. A disadvantage of this system is a high production cost and difficulties related with a faultless construction of such matrix.

The device presented in the work (Ermert et al., 2000) uses a linear sending probe, composed of 128 piezoceramic transducers, of rectangular dimensions (width much larger than height), a linear receiving probe, composed of 128 PVDF transducers (height much larger than width) and a lens, which focuses an ultrasonic wave beam in one direction. Probes work in the frequency range of 2 ÷ 4 MHz. Sweeping of the structure of an object located in water, between probes, is realised by the means of phase focusing of an ultrasonic wave beam in the object plane, in the form of horizontal lines, 1.25 mm wide, which, after a

transition through the object and the lens, are received by proper linear transducers of the receiving probe. One disadvantage in this case is beam focusing in a particular area of the object, what causes image spreading and occurrence of artefacts outside the focus.

The device presented in work (Lehmann et al., 1999) is a model of an acoustic holograph used the through-transmission signal. This approach uses coherent sound and coherent light to produce real-time, large field-of-view images with pronounced edge definition in soft tissues of the body.

In most of known studies, the projection parameter is the signal amplitude, not its transition time, which seems to more attractive due to the simplicity and precision of measurements.

This Section (8) includes a description of the results of author's studies, which aim is a construction of a special measuring setup for visualisation of biological structures by the means of ultrasonic projection, which enables simultaneous measurements of several acoustic parameters in pseudo-real time (multi-parameter ultrasonic transmission camera), using a pair of electronically controlled multi-element matrices of piezoceramic transducers, described in Section 7.

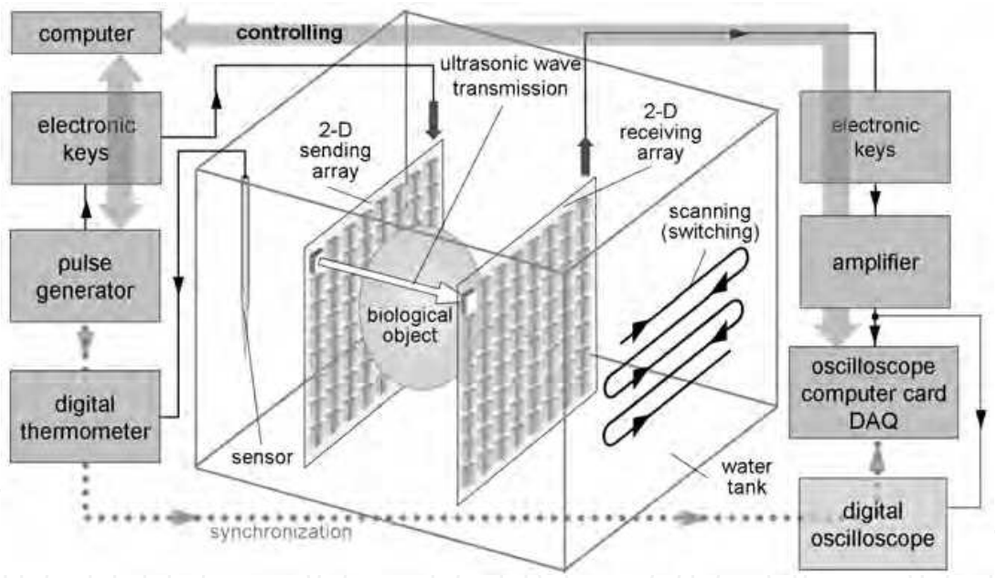


Fig. 21. Block scheme of the laboratory measurement setup for visualization of the distribution of acoustic parameters of biological media internal structure by means of ultrasonic projection method

Due to diversified ways of conducting electrodes to transducers of matrices and different controlling methods, two laboratory setups were developed, for imaging internal structures of biological media, by the means of ultrasound projection: using a pair of ultrasonic 512—element standard matrix – sending and receiving one - and using a pair of ultrasonic 512-element passive or active matrices (Opielinski & Gudra, 2010a; Opielinski et al., 2010a, 2010b). A general block scheme of the laboratory measurement setup is presented in Fig.21. Elementary piezoceramic transducers of the sending matrix (Opielinski & Gudra, 2010a) are excite by a burst type pulses generator, controlled by a computer through the GPIB

connection. A computer is also used for switching transducers of sending and receiving matrices, using developed and software-assisted systems of electronic keys. Signals received by elementary piezoceramic transducers of the receiving matrix (Opielinski & Gudra, 2010a) after an amplification and acquisition by the means of a computer oscilloscope data acquisition (DAQ) card, are recorded on the hard drive. Additionally, a digital oscilloscope is used for visualisation and control of measurement signals. Projection values of acoustic parameters assigned for visualisation (e.g. transition time of an ultrasonic wave or a projective value of sound velocity) are determined from recorded signals, by the means of a specially developed software. Water temperature is controlled by a digital thermometer of the resolution at 0.1 °C. The acceleration of measurements, e.g. by decreasing sampling frequency of receiving signal, enables to obtain images in pseudo-real time (several to ten-odd frames per second). It can be used simple square burst pulse generator as integrated electronic circuit instead sinusoidal one, what enables to achieve the amplitude of ultrasonic matrix transducer exciting signal more than 60 $V_{pp}$, as well.

One of objects that were subjected to projection examinations on the developed measurement setups, was phantom *AC_Blue* in the form of a cylinder made of agar gel, of the diameter of 55 mm and the length of 50 mm, made of 3 % (by weight) agar solution, with an additive of propylene glycol (by volume), in order to achieve a greater diversification of sound velocity values in the structure in relation to the values in water (Fig.22a). Two cylinders, made of about 4 % agar solution with an additive of propylene glycol, were decentrally put into the cylinder. Diameters of internal cylinders were 15 mm and 8 mm. Additionally, in the *AC_Blue* cylinder, a through-and-through round hole, of 6 mm diameter, was made. This hole was filled with water during measurements. Sound velocities in the structure of *AC_Blue* cylinder are different from the speed in water, by the following values: +10 m/s – surroundings, +13 m/s larger internal cylinder, +12 m/s smaller internal cylinder. Figure 22b presents, in grey scale, an image of the distribution of projection values of sound velocity in a lateral projection of agar phantom *AC_Blue*, obtained from measurements, made using a pair of 512-element standard matrices (Section 7.1) in the resolution of 32 x 16 pixels.

Figure 23a presents an image (in grey scale) of the distribution of the projection values of sound velocity in longitudinal projection of a hard-boiled chicken egg, without shell, immersed in water, obtained from measurements, made using a pair of 512-element passive matrices, in the resolution of 32 x 16 pixels. A similar image of the distribution of frequency of ultrasonic wave pulses in a longitudinal projection of the same egg is presented in Figure 23b.

Heterogeneities, differing in sound velocities values even by about several m/s are clearly visible in projection images (Fig.22). On the basis of these images, it is possible to estimate sound speeds in the structure of examined objects. The projection image of a hard-boiled egg (Fig.23) distinctly visualises borders of the yolk area. Images obtained from projection measurements of a frequency down shift of receiving pulses (Fig.23b) are of a worse quality than images visualising projections of sound velocity (Fig.23a), however, it is not difficult to clearly recognise heterogeneity boundaries in both images. The higher is attenuation in a medium on the way of an ultrasonic wave beam, the larger is drop of frequency of a receiving pulse (formula (4); see Fig.23b).

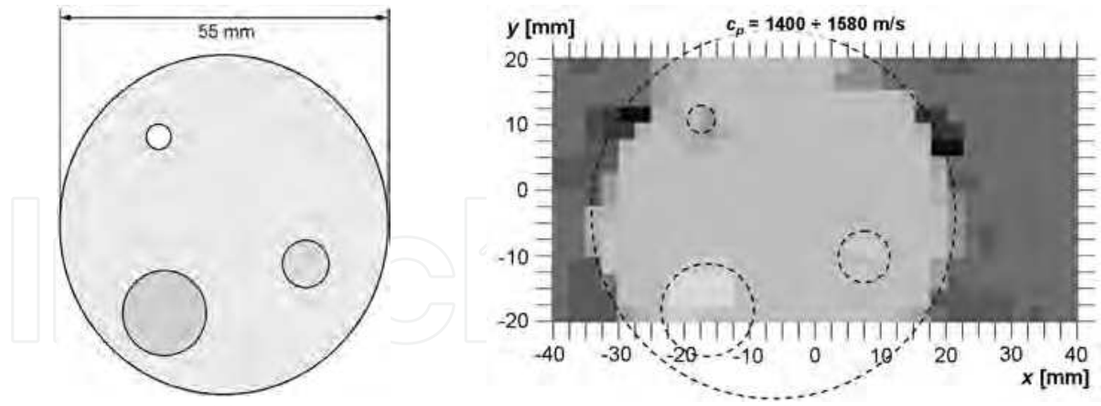


(a) (b)

Fig. 22. Lateral projection of the agar phantom *AC_Blue*: structure (a), image of the distribution of projection values of sound velocity in grey scale (b)

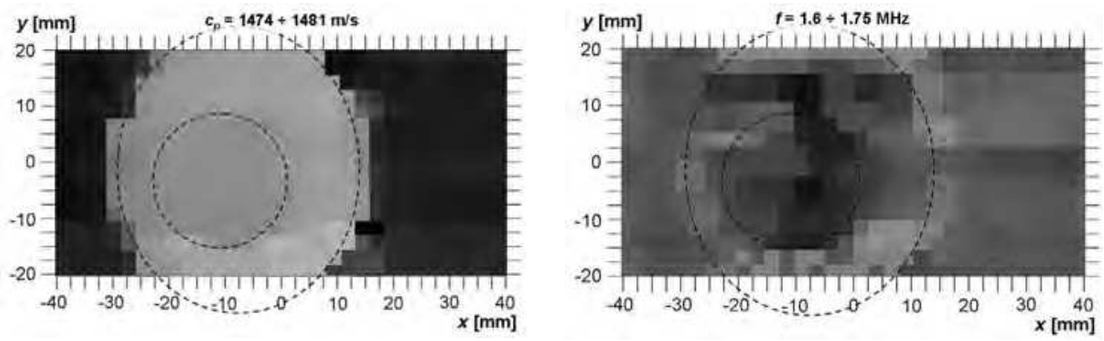


(a) (b)

Fig. 23. An image of the distribution of the projection values of sound velocity in a longitudinal projection of a hard-boiled chicken egg (a) and an image of the distribution of the projection values of frequency of receiving pulses in a longitudinal projection of the same egg (b)

Good image quality without artefacts caused by the beam focusing is a great advantage in that solution in comparison with UTC described in literature (Brettel et al., 1981; Ermert et al., 2000; Granz & Oppelt, 1987; Green et al., 1974). The disadvantage is not so good scanning resolution, at present, what have to be improved.

## 9. Summary

The results obtained confirm that the designed multi-element ultrasonic 2-D matrices are suitable for projection imaging of biological media (especially soft tissue) with the use of scanning method through switching of the right pairs (or groups) of sending and receiving elementary transducers. Using appropriate combinations of apertures of the sending and receiving matrix (with accordance to the scanning method) allows to increasing the directivity and the acoustic pressure level of the ultrasonic wave beam and ensures its apodization in the transmission system. Additionally, rotation of a pair of probes around the

studied biological object submerged in water will allow tomographic, three dimensional reconstruction of its internal structure.

In order to improve the quality of ultrasound projection images, there are currently conducted research works on developing constructions of ultrasonic matrices and the ultrasonic transmission camera set-up. In order to increase scanning resolution, it is planned to develop ultrasonic matrices with elementary transducers of smaller sizes, circular-shaped, in a higher amount and arranged more densely.

## 10. References

Brettel, H.; Roeder, U. & Scherg, C. (1981). Ultrasonic Transmission Camera for Medical Diagnosis, *Biomedizinische Technik*, Vol. 26, No. s1, pp. 135-136, ISSN 0013-5585

Brettel, H.; Denk, R.; Burgetsmaier, M. & Waidelich, W. (1987). Transmissionssonographie, In: *Ultraschalldiagnostik des Bewegungsapparates*, T.Struhler & A.Feige (Ed.), pp. 246-251, Springer Verlag, ISBN 3540166920, Berlin, Heidelberg, New York, London, Paris, Tokyo

Chiao, R.Y. & Thomas, L.J. (1996). Aperture formation on reduced-channel arrays using the transmit-receive apodization matrix, *1996 IEEE Ultrasonics Symposium Proceedings*, ISBN 0-7803-3615-1, San Antonio, USA, November 1996

Drinkwater, B.W. & Wilcox, P.D. (2006). Ultrasonic arrays for non-destructive evaluation: A review, *NDT&E International*, Vol. 39, No. 7, pp. 525-541, ISSN 0963-8695

Eames, M.D.C. & Hossack, J.A. (2008). Fabrication and evaluation of fully-sampled, two-dimensional transducer array for "Sonic Window" imaging system, *Ultrasonics*, Vol. 48, pp. 376-383, ISSN 0041-624X

Ermert, H.; Keitmann, O.; Oppelt, R.; Granz, B.; Pesavento, A.; Vester, M.; Tillig, B. & Sander, V. (2000). A New Concept For a Real-Time Ultrasound Transmission Camera, *IEEE Ultrasonics Symposium Proceedings*, ISBN 0-7803-6365-5, San Juan, Puerto Rico, October 2000

Granz, B. & Oppelt, R. (1987). A Two Dimensional PVDF Transducer Matrix as a Receiver in an Ultrasonic Transmission Camera, *Acoustical Imaging*, Vol. 15, pp. 213-225, ISSN 0270-5117

Green, P.S.; Schaefer, L.F.; Jones, E.D. & Suarez, J.R. (1974). A New High Performance Ultrasonic Camera, *Acoustical Holography*, Vol. 5, pp. 493-503, ISSN 0065-0870

Green, P.S.; Schaefer, L.F.; Frohbach, H.F. & Suarez, J.R. (1976). *Ultrasonic Camera System and Method*, US Patent 3937066.

Greenleaf, J.F. & Sehgal, Ch.M. (1992). *Biologic System Evaluation with Ultrasound*, Springer-Verlag, ISBN 0387978518, 3540978518, New York, USA

Hoctor, R.T. & Kassam, S.A. (1990). The Unifying Role of the Coarray in Aperture Synthesis for Coherent and Incoherent Imaging, *Proceedings of the IEEE*, Vol. 78, No. 4, pp. 735-752, ISSN 00189219

Johnson, J.A.; Karaman, M. & Khuri-Yakub B.T. (2005). Coherent-Array Imaging Using Phased Subarrays. Part I: Basic Principles, *IEEE Transactions on Ultrasonics, Ferroelectrics, and Frequency Control*, Vol. 52, No. 1, pp. 37-50, ISSN 0885-3010

Kak, A.C & Slaney, M. (1988). *Principles of Computerized Tomographic Imaging*, IEEE Press, ISBN/ASIN 0879421983, New York, USA

Karaman, M.; Wygant, I.O.; Oralkan, O. & Khuri-Yakub, B.T. (2009). Minimally Redundant 2-D Array Design for 3-D Medical Ultrasound Imaging, *IEEE Transactions on Medical Imaging*, Vol. 28, No. 7, pp. 1051-1061, ISSN 0278-0062

Keitmann, O.; Benner, L.; Tillig, B.; Sander, V. & Ermert, H. (2002). New Development of an Ulrasound Transmission Camera, *Acoustical Imaging*, Vol. 26, pp. 397-404, ISBN 0306473402 / 0-306-47340-2

Kim, J-J. & Song, T-K. (2006). Real-Time High-Resolution 3D Imaging Method Using 2D Phased Arrays Based on Sparse Synthetic Focusing Technique, *2006 IEEE Ultrasonics Symposium Proceedings*, ISBN 9781424402014, Vancouver, Canada, October 2006

Lehmann, C.D.; Andre, M.P.; Fecht, B.A.; Johannsen, J.M.; Shelby, R.L. & Shelby, J.O. (1999). Evaluation of Real-Time Acoustical Holography for Breast Imaging and Biopsy Guidance, *SPIE Proceedings*, Vol. 3659, pp. 236-243, ISBN 0-8194-3131-1, San Diego, USA, May 1999

Lockwood, G.R. & Foster, F.S. (1996). Optimizing the Radiation Pattern of Sparse Periodic Two-Dimensional Arrays, *IEEE Transactions on Ultrasonics, Ferroelectrics, and Frequency Control*, Vol. 43, No. 1, pp. 15-19, ISSN 0885-3010

Narayana, P.A. & Ophir, J. (1983). A Closed Form Method for the Measurement of Attenuation in Nonlinearly Dispersive Media, *Ultrasonic Imaging*, Vol. 5, No. 1, pp. 17-21, ISSN 0161-7346

Nowicki, A. (1995). *Basis of Doppler Ultrasonography*, PWN, ISBN 83-01-11793-1, Warsaw, Poland (in Polish)

Nowicki, A.; Wójcik, J. & Kujawska, T. (2009). Nonlinearly Coded Signals for Harmonic Imaging, *Archives of Acoustics*, Vol. 34, No. 1, pp. 63-74, ISSN 0137-5075

Opielinski, K. & Gudra, T. (2000). Ultrasound Transmission Tomography Image Distortions Caused by the Refraction Effect, *Ultrasonics*, Vol. 38, No. 1-8, pp. 424-429, ISSN 0041-624

Opielinski K.J. & Gudra T. (2004). Three-Dimensional Reconstruction of Biological Objects' Internal Structure Heterogeneity from the Set of Ultrasonic Tomograms, *Ultrasonics*, Vol. 42, No. 1-9, pp. 705-711, ISSN 0041-624

Opielinski, K.J. & Gudra, T. (2004). Ultrasonic Transmisson Camera: *Proceedings of LI Open Seminar on Acoustics*, ISBN 83-87280-35-6, Gdansk-Sobieszewo, Poland, September 2004 (in Polish)

Opielinski, K.J. & Gudra, T. (2004). Biological Structure Imaging by Means of Ultrasonic Projection, In: *Acoustical Engineering: Structures – Waves – Human Health*, Vol. 13, No. 2, R.Panuszka (Ed.), pp. 97-106, Polish Acoustical Society, Krakow, Poland

Opielinski, K.J. & Gudra, T. (2005). Computer Recognition of Biological Objects' Internal Structure Using Ultrasonic Projection, *Computer Recognition Systems*, pp. 645-652, ISSN 1615-3871

Opielinski, K.J. & Gudra, T. (2006). Multi-Parameter Ultrasound Transmission Tomography of Biological Media, *Ultrasonics*, Vol. 44, No. 1-4, pp. e295-e302, ISSN 0041-624X

Opielinski, K.J. (2007). Ultrasonic Parameters of Hen's Egg, *Molecular and Quantum Acoustics*, Vol. 28, pp. 203-216, ISSN 1731-8505

Opielinski, K. & Gudra, T. (2008). Nondestructive Tests of Cylindrical Steel Samples using the Ultrasonic Projection Method and the Ultrasound Transmission Tomography

Method, *Acoustics '08*, ISBN 9782952110549 2952110549, Paris, France, June/July 2008

Opielinski, K.J.; Gudra, T. & Pruchnicki, P. (2009). *The Method of a Medium Internal Structure Imaging and the Device for a Medium Internal Structure Imaging*, Patent Application No. P389014, Wroclaw University of Technology, Poland (in Polish).

Opielinski, K.J. & Gudra, T. (2010). Multielement Ultrasonic Probes for Projection Imaging of Biological Media, *Physics Procedia*, Vol. 3, No. 1, pp. 635-642, ISSN 18753892

Opielinski, K.J. & Gudra, T. (2010). Ultrasonic Transmission Tomography, In: *Industrial and Biological Tomography – Theoretical Basis and Applications*, J.Sikora & S.Wojtowicz (Ed.), Electrotechnical Institute, ISBN 978-83-61956-04-4, Warsaw, Poland

Opieliński, K.J. & Gudra, T. (2010). Aperture Synthesis on 2-D Ultrasonic Transducer Arrays for Projection Imaging of Biological Media, *Proceedings of 20th International Congress on Acoustics ICA 2010*, Sydney, Australia, August 2010

Opielinski, K.J.; Gudra, T. & Pruchnicki, P. (2010). Narrow Beam Ultrasonic Transducer Matrix Model for Projection Imaging of Biological Media, *Archives of Acoustics*, Vol. 35, No. 1, pp. 91-109, ISSN 0137-5075

Opielinski, K.J.; Gudra T. & Pruchnicki, P. (2010). A Digitally Controlled Model of an Active Ultrasonic Transducer Matrix for Projection Imaging of Biological Media, *Archives of Acoustics*, Vol. 35, No. 1, pp. 75-90, ISSN 0137-5075

Ramm von, O.T. & Smith, S.W. (1983). Beam Steering with Linear Arrays, *IEEE Transaction Biomedical Engineering*, Vol. BME-30, No. 8, pp. 438-452, ISSN 0018-9294

Thomenius, K.E. (1996). Evolution of Ultrasound Beamformers, *1996 IEEE Ultrasonics Symposium Proceedings*, Vol. 2, ISBN 0-7803-3615-1, San Antonio, USA, November 1996

Wildes, D.G.; Chiao, R.Y.; Daft, Ch.M.W.; Rigby K.W.; Smith L.S. & Thomenius, K.E. (1997). Elevation Performance of 1.25D and 1.5D Transducer Arrays, *IEEE Transactions on Ultrasonics, Ferroelectrics, and Frequency Control*, Vol. 44, No. 5, pp. 1027-1037, ISSN 0885-3010

Wygant, I.O.; Karaman, M.; Oralkan, O. & Khuri-Yakub, B.T. (2006). Beamforming and Hardware Design for a Multichannel Front-End Integrated Circuit for Real-Time 3D Catheter-Based Ultrasonic Imaging, *SPIE Medical Imaging*, Vol. 6147, pp. 61470A-1-8, ISBN 9780819471048

Wygant, I.O.; Lee, H.; Nikoozadeh, A; Yeh, D.T.; Oralkan, O.; Karaman, M. & Khuri-Yakub, B.T. (2006). An Integrated Circuit with Transmit Beamforming and Parallel Receive Channels for Real-Time Three-Dimensional Ultrasound Imaging, *2006 IEEE Ultrasonics Symposium Proceedings*, ISBN 9781424402014, Vancouver, Canada, October 2006

Yen, J.T. & Smith, S.W. (2004). Real-Time Rectilinear 3-D Ultrasound Using Receive Mode Multi-plexing, *IEEE Transactions on Ultrasonics, Ferroelectrics, and Frequency Control*, Vol. 51, No. 2, pp. 216-226, ISSN 0885-3010

Zhang, D.; Gong, X.; Rui, B.; Xue, Q. & Li, X. (1997). Further Study on the Nonlinearity Parameter Tomography for Pathological Porcine Tissues, *Proceedings of Ultrasonics World Congress WCU'97*, ISBN 4-9900616-0-8, Yokohama, Japan, August 1997

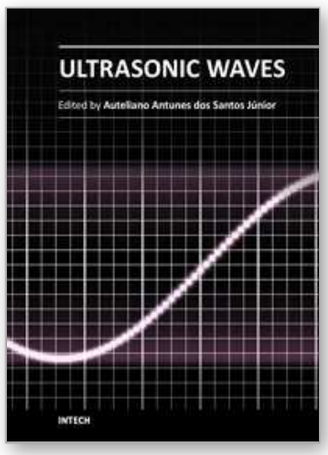


**Ultrasonic Waves**
Edited by Dr Santos

ISBN 978-953-51-0201-4
Hard cover, 282 pages
**Publisher** InTech
**Published online** 07, March, 2012
**Published in print edition** March, 2012

Ultrasonic waves are well-known for their broad range of applications. They can be employed in various fields of knowledge such as medicine, engineering, physics, biology, materials etc. A characteristic presented in all applications is the simplicity of the instrumentation involved, even knowing that the methods are mostly very complex, sometimes requiring analytical and numerical developments. This book presents a number of state-of-the-art applications of ultrasonic waves, developed by the main researchers in their scientific fields from all around the world. Phased array modelling, ultrasonic thrusters, positioning systems, tomography, projection, gas hydrate bearing sediments and Doppler Velocimetry are some of the topics discussed, which, together with materials characterization, mining, corrosion, and gas removal by ultrasonic techniques, form an exciting set of updated knowledge. Theoretical advances on ultrasonic waves analysis are presented in every chapter, especially in those about modelling the generation and propagation of waves, and the influence of Goldberg's number on approximation for finite amplitude acoustic waves. Readers will find this book ta valuable source of information where authors describe their works in a clear way, basing them on relevant bibliographic references and actual challenges of their field of study.

**How to reference**
In order to correctly reference this scholarly work, feel free to copy and paste the following:

Krzysztof J. Opieliński (2012). Ultrasonic Projection, Ultrasonic Waves, Dr Santos (Ed.), ISBN: 978-953-51-0201-4, InTech, Available from: http://www.intechopen.com/books/ultrasonic-waves/ultrasonic-projection

INTECH
open science | open minds

**InTech Europe**
University Campus STeP Ri
Slavka Krautzeka 83/A
51000 Rijeka, Croatia
Phone: +385 (51) 770 447
Fax: +385 (51) 686 166
www.intechopen.com

**InTech China**
Unit 405, Office Block, Hotel Equatorial Shanghai
No.65, Yan An Road (West), Shanghai, 200040, China
中国上海市延安西路65号上海国际贵都大饭店办公楼405单元
Phone: +86-21-62489820
Fax: +86-21-62489821

IntechOpen